International Journal of Modern Manufacturing Technologies
ISSN 2067–3604, Vol. XII, No. 1 / 2020

SIMULATION OF PROPERTIES OF DISSIMILAR WELDED JOINTS OF DUPLEX 2205 AND AUSTENITIC 316L STEELS

Santina Topolska[2], Aleksander Gwiazda[1]

[1] Silesian University of Technology, Faculty of Mechanical Engineering, Institute of Engineering Processes Automation and Integrated Manufacturing Systems
Konarskiego 18A, 44-100 Gliwice, Poland
[2] Silesian University of Technology, Faculty of Mechanical Engineering, Institute of Engineering Materials and Biomaterials
Konarskiego 18A, 44-100 Gliwice, Poland

Corresponding author: Aleksander Gwiazda, aleksander.gwiazda@polsl.pl

Abstract: The article presents the computer aided simulation of mechanical properties of dissimilar welded joints based on duplex 2205 and austenitic 316L stainless steels manufactured using austenitic binder. The purpose of researches was to analyze the impact of joint type and binder material on the mechanical properties of these welded joints. The duplex stainless steel has given its name to the similarity (in terms of processing and physical properties) to ferritic steels and (in terms of chemical composition and excellent corrosion resistance) to austenitic steels. The duplex family already includes more than 40 steel grades that are constantly being developed. The combination of chromium, molybdenum, nitrogen and tungsten provides corrosion resistance significantly better than in the case of acid-resistant steels according to AISI 314 standard, and additionally these steels are characterized by higher strength (at room temperature almost twice the tensile strength). The aim of the work is to develop a method for modeling welded welds in FEM calculations and numerical calculation methodologies that allow for the strength of such welds and their nonlinear properties.
Key words: Welded joints, duplex steels, simulation

1. INTRODUCTION

Duplex steel is a type of ferritic-austenitic steel in which ferrite phase and austenite phase occur in a significant volume (within 50%). Duplex steels exhibit the constant average yield point R0.2 of 450-500 MPa [1]. Such high mechanical properties (for example in relation to 316L steels) are due to two factors: first, fine-grained structure and, secondly, the presence of intergranular nitrogen solution in austenite. It should be noted that almost all of the nitrogen content in the steel is dissolved only in the austenite and thus the properties of this phase are increased, reaching the same strength as the ferrite one. It should also be noted that in duplex steels the yield point is usually two times lower than the tensile strength [2]. Cold forming of semi-finished products may result in a significant increase of the yield point of duplex steels. This is related to the greater strength of the two-phase structure. Higher hardness means that duplex steels are characterized by a higher resistance to abrasive wear and erosion. Another factor that increases the hardness of this steel is the chemical composition, and above all, the occurrence of the main alloying elements [3-5].

One of the characteristic features of duplex steel is their high corrosion resistance [6, 7]. Even the lean (2304) duplex steel shows higher resistance than average austenitic steels. Whereas, the corrosion resistance of the superduplex steel (2507) is significantly higher. Distinctive is the comparison of the mechanical properties and corrosion resistance of these two groups of steels. Mechanical properties are determined by the yield point values R0,2 while corrosion resistance is expressed by the Critical Pitting Temperature (CPT) value. The conducted analyzes confirm that with similar corrosion resistance parameters (CPT), duplex steels show around two times higher mechanical properties. Furthermore, taking into account one of the basic corrosive environments, which is the chloride one, one can point to even much more visible resistance of duplex steels.

The basic parameters determining the corrosion resistance of steel are, as it was stated: critical pitting corrosion temperature (CPT) and critical crevice corrosion temperature (CCT - Critical Crevice Temperature, or sometimes CCCT - Critical Crevice Corrosion Temperature). Corrosion resistance to chloride ions depends on their concentration and temperature. For example, it can be stated that for austenitic steel 316L, the CPT parameter is about 10°C and the CCT one about - 10°C [8]. However, in the case of the hyperduplex 2707 steel, these parameters are 98°C and 70°C respectively.

It should be noted that in comparison to austenitic steels, duplex steels show high corrosion resistance, especially in high pH environments [9]. This applies to

inorganic acids (sulfuric acid (VI) and also nitric acid (V)) as well as organic acids (formic acid and acetic acid). In the presence of reducing acids the main role in the corrosion resistance of these steels plays their ability to passivity. However, in the presence of oxidizing acids, the corrosion resistance of duplex steel is the result of the corrosion resistance of the passivation layer itself [10, 11]. Such high corrosion resistance is also the result of both the two-phase structure and the effect of alloying elements. Among the alloying elements, Cr, Mo and N are the most important. These elements have the greatest impact on pitting corrosion resistance, and to a lesser extent, on crevice corrosion. Duplex steels are also characterized by significantly higher resistance to stress corrosion than austenitic steels of similar CPT value, especially at higher temperatures.

2. RESEARCH METHODOLOGY

2.1 Specimens

For the research, four types of butt joints were prepared. They are divided into two groups: two-pass welds and multiple-pass welds. The chosen joints were (Figure 1):

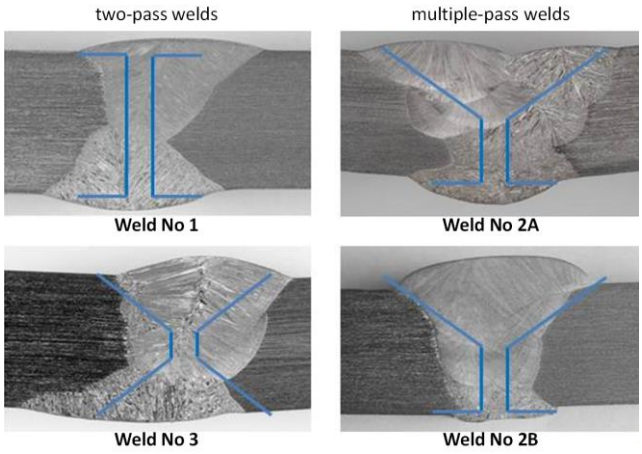

Fig. 1. Investigated types of dissimilar welded joints (2205 – 316L), [own elaboration]

Welding process was performed using the 3.2 mm AVESTA P5 welding wire. This wire characterizes with the austenitic structure containing 5 - 10% of ferrite (EN ISO 14343: S 23 12 2 L, AWS A5.9: ER309LMo).

Table 1. Chemical composition of welded materials (%), [own elaboration]

	C	Si	Mn	Cr	Ni	Mo	N
2205	0.027	0.41	0.80	22.8	5.33	3.11	0.16
316L	0.041	0.52	1.69	17.2	9.90	2.10	0.04
AVESTA P5 S 23 12 2 L	0.009	0.32	1.4	21.2	15.1	2.62	0.06

The ferrite number for the AVESTA P5 welding wire is 8 (according deLong diagram) or 9 (according the WRC-92 diagram) [12]. Values of the heat input, during welding, varied between 1.19 kJ/mm (weld No 2A) to 3.64 kJ/mm (weld No 2B).

2.2. Toughness tests

Toughness tests were carried out using specimens prepared in accordance with the scheme shown in Figure 2(localization of all specimens). The temperature during the toughness test was -40°C. This temperature value was chosen, because the vast majority of industrial structures of the tested type usually work in higher temperature ranges (except for extreme temperatures, but they concern special constructions).

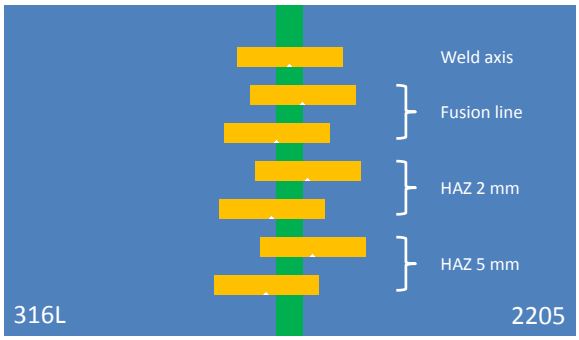

Fig. 2. Localization of specimens for the toughness tests, [own elaboration]

The results of fracture energy measurements of all investigated specimens are presented in a compact form in Figure 3. On the left side of the horizontal axis are values of energy needed to fracture specimens with the V-notch on the 2205steel side, while on the right side energy values for the specimens with the V-notch on 316L steel side. In the case of the joint No 1, the lowest value of fracture energy is observed for the specimen with the notch in the axis of the weld (94 J). The highest fracture energy value was recorded in the case of the HAZ 2 316L (273 J) specimen. For the joint No 2A, the lowest value of the fracture energy is 106 J (weld axis), and the highest is 243 (HAZ 2 316L). For the joint No 2B, respectively, the lowest value is 74 J (FL 2205) and the highest one is 245 J (HAZ 5 316L). For the joint No 3, the lowest fracture energy value is observed for the specimen with the notch in the fusion line on the 2205steel side (FL 2205) and is 152 J. The highest value is 242 J for the specimen with the notch located 5 mm from the fusion line on the 316L steel side (HAZ 5 316L).

The presented analysis allows elaborating comparative results of toughness tests (fracture energy) of individual parts of welded joints being tested. Generally, the highest, average, fracture energy value is observed in the case of the joint No 3 (204.2 J) and in the case of the joint No 2A (203.5 J). Thus, these two types of connectors should be considered the most toughness.

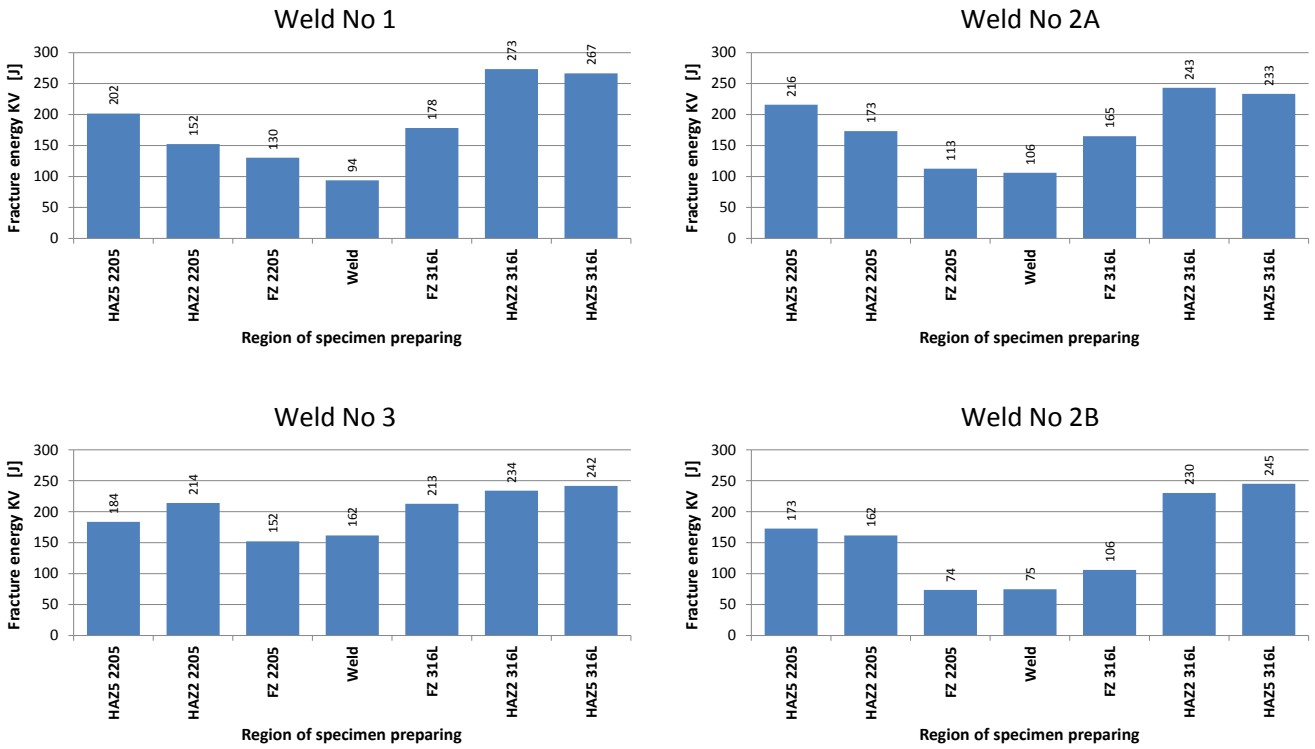

Fig. 3. Investigated types of dissimilar welded joints (2205 – 316L), [own elaboration]

Tests results of fracture energy for specimens from the area of HAZ 2205 indicate the higher average measurement for the joint No 2A before measurements for the joint No 3.

The characteristics resulting from the comparison of the average fracture energy for the weld area (middle) are slightly different then for the specimens of the HAZ 2205 area. In this case dominates the joint No 3 before joints No 1 and No 2A, which have comparable results. Only in the case of analyzing the fracture energy for the specimens with the notch on the side of HAZ 316L one can observe the dominance of the joint No 1 over the others (by about 12%).

3. VIRTUAL SPECIMEN TESTS

To elaborate the model of the fracture process of the weld the virtual model has been elaborated. The objective of this stage of investigations is to elaborate the methodology of virtual specimens preparation that allow obtaining fairly reliable information about stresses and strains in the area of such type welded joint. In Figure 4 is presented the investigated model of the joint. All material characteristics of the model are based on the metallographic investigations and tests of mechanical properties. In Figures 5 and 6 are presented results of the strains analysis as a result of crosswise force acting.

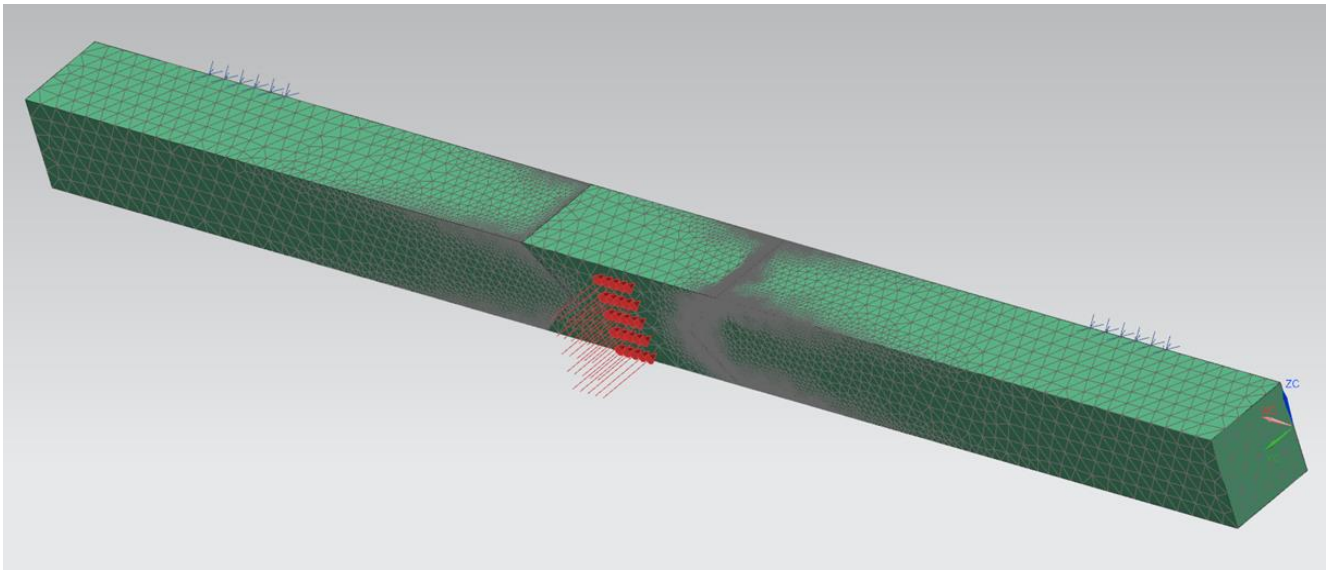

Fig. 4. Virtual model of the dissimilar welded joint (2205 – 316L), [own elaboration]

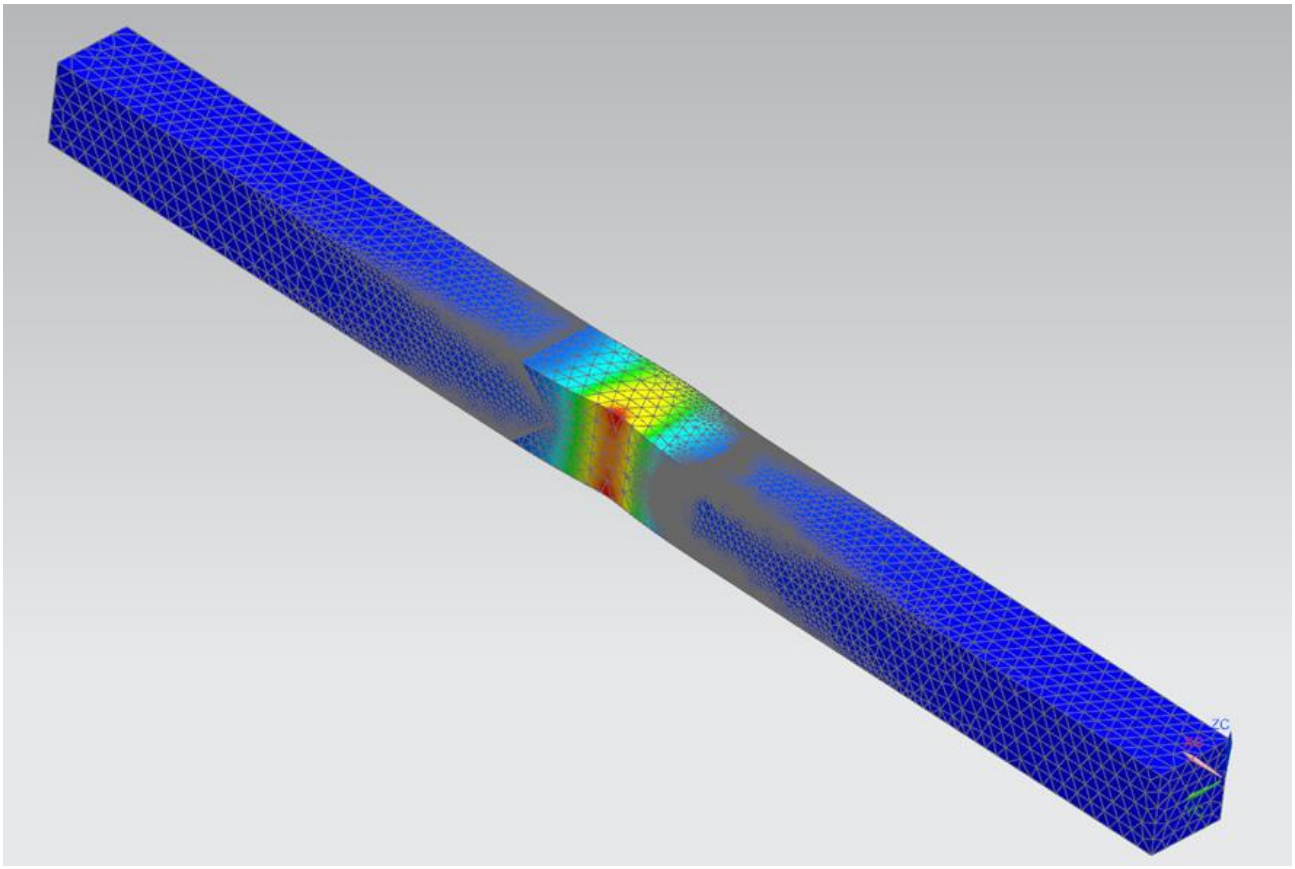

Fig. 5. Strains of the specimen of the welded joint (316L - 2205) during axial force acting, [own elaboration]

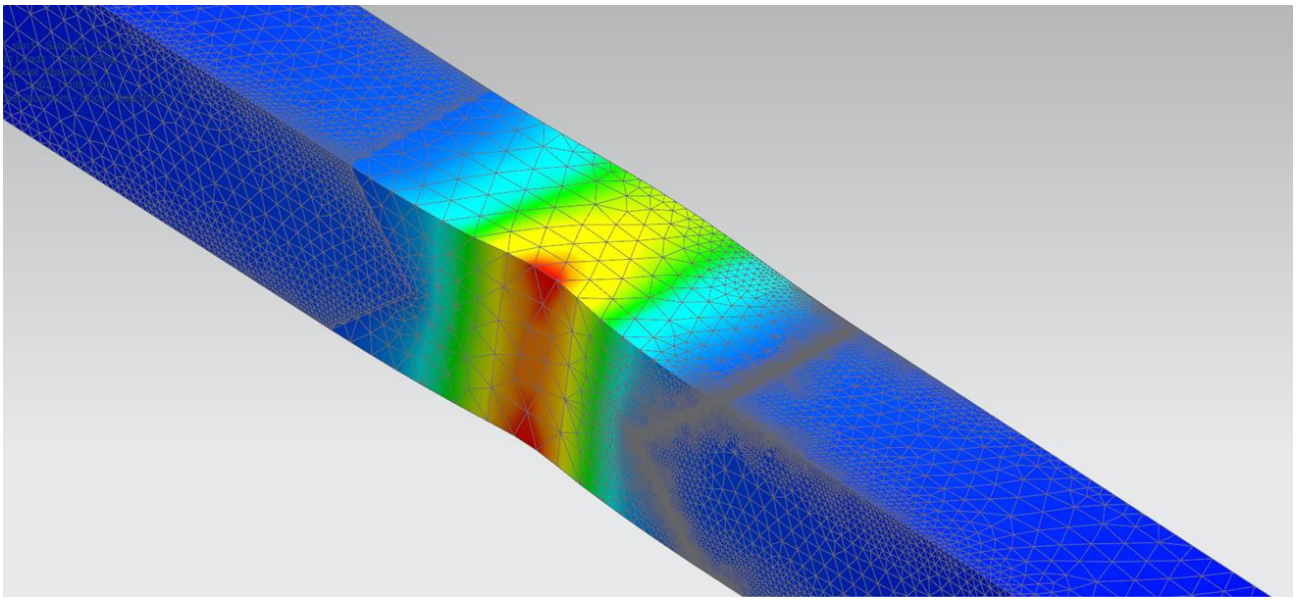

Fig. 6. The area of the weld from the Figure 5, [own elaboration]

The prepared model was used to conduct the analysis of stress distribution in the area of the joint. Such analyses are rare in bibliography. They are mainly focused on thermal processes and stress distribution of homogenous modeled joints [13-17]. In the paper the joint was modeled basing on the metallographic investigations and the results of the mechanical properties tests. Then the model was used to simulate the stress distribution during the crosswise load acting like during toughness tests.

To analyze all relation concerning the elaborated model it was decided to investigate the behavior, during virtual tests, the simplified model of the specimen, but including the different approaches to model the particular parts of the joint: weld zone, HAZ'es and base materials.

In Figure 7 is presented the stress distribution in the joint area and around the particular HAZ zones, wherein these images represent the stress distribution inside the specimen.

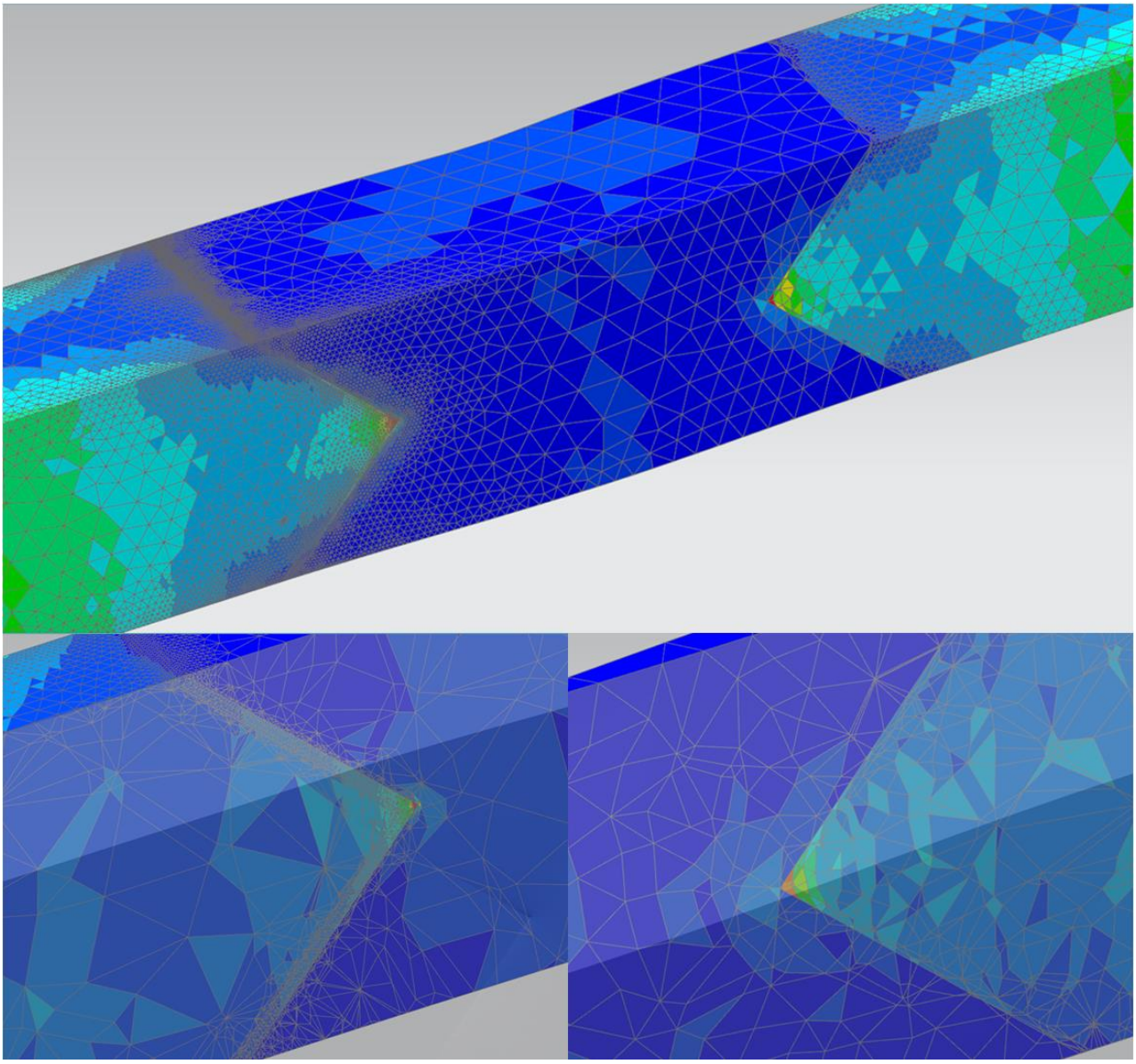

Fig. 7. Stress distribution around the joint zone (2205 – 3016L), [own elaboration]

4. ANALYSIS OF TEST RESULTS

The results of the virtual tests as well as of the toughness tests show that there is a large convergence between these outcomes. Microscopic observations confirm the results of investigations of mechanical properties of the grain size of main phases and the nature of the created dendrites. The average width of HAZ 2205 is greater than the average width of HAZ 316L. The width of HAZ 2205 varies between 200 and 400 μm. In the virtual model the HAZ 2205 was modeled with the width of 300 μm. The width of the HAZ 316L varies between 50 and 150 μm (in the model it is equal to 150 μm). In the case of joints welded with lower linear energies, dendrites are less densely packed and are usually columnar ones what was considered in the mechanical properties of the model material. One of the causes of the observed fracture in the HAZ 2205 area is the precipitation of $M_{23}C_6$ carbides (these precipitations are shown in Figure 8). It must be said that this precipitation is particularly dangerous in the case of stress corrosion, with fractures similarly in the HAZ 2205 zone.

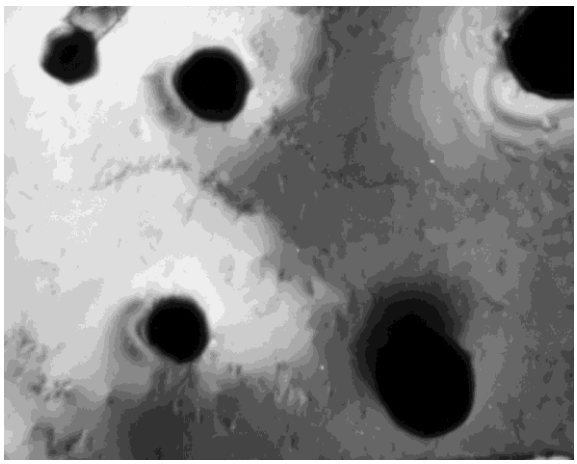

Fig. 8. $M_{23}C_6$ carbides in the matrix of the γ phase, [own elaboration]

The conducted tests of the virtual model show that there is important to model the particular components of such joints basing on the material parameters obtained during metrical tests of real specimens to elaborate the reliable base of material characteristics.

5. CONCLUSIONS

Some conclusions can be drawn from the present study. Generally the tests of mechanical characteristics confirm good properties of analyzed type of welded joints. The highest average fracture energy value is characteristic for the joint No 3, and the lowest for the joint No 2B (the difference by 20%). Other joints are characterized by fracture energy close to the highest (differences of 1 and 0,5%, respectively). This confirms the negative correlation between the amount of heat introduced into the weld (including welding energy) and the toughness of the welded joints. In addition, it should be noted that the highest toughness is shown in the case of the notch location on the HAZ 316L side (KV on average 246 J), and the lowest for specimens with notches in the weld area (KV on average 131 J).

Analyzing the area of the fracture it should be stated that the most probable place is HAZ 2205. It is related with the morphology of this zone (a lot of different types of carbides precipitates). The analysis of the virtual test, using the model with material characteristics based on the metallographic analysis and toughness test also show that in this area it is observed the stress concentration.

Basing on the presented results it is planned to elaborate the method of modeling the dissimilar joints of this type (duplex – austenitic steels) to predict its future properties.

6. REFERENCES

1.Gunn, R. N., (2003). *Duplex Stainless Steels: Microstructure, Properties and Applications*, (Cambridge: Abington Publishing).

2.Nowacki, J., (2009). *Duplex steel and its weldability* Wydawnictwa Naukowo - Techniczne, Warszawa (in Polish).

3.Adamiak, M., Czupryński, A., Kopyść, A., Monica, Z., Olender, M., Gwiazda, A., (2018). *The Properties of Arc-Sprayed Aluminum Coatings on Armor-Grade Steel*, Metals, **8**(2), pp. 1-10, DOI:10.3390/met8020142

4.Alvarez-Armas, I., Degallaix-Moreuil, S. (eds.), (2009). *Duplex Stainless Steels*, (Hoboken: John Wiley & Sons).

5.Davies, J. R. (ed.), (2016). *Corrosion of Weldments*, ASM International, Materials Park.

6.Schweitzer, Ph. A., (2007). *Fundamentals of Metallic Corrosion: Atmospheric and Media Corrosion of Metals*, CRC Press, Boca Raton.

7.Kocijan, A., Donik, C., Jenko, M., (2009). The Corrosion Behaviour of Duplex Stainless Steel in Chloride Solutions Studied by XPS, Mat. and Tech., **43**(4), pp. 195–199.

8. *Sandvik SAF 2507*. Available from: http://smt.sandvik.com/en/materials-center/material-datasheets/tube-and-pipe-seamless/sandvik-saf-2507/. Accessed: 11/04/2019.

9.Garverick, L. (red.), (1994). *Corrosion in the Petrochemical Industry*, ASM International, Materials Park.

10.Sherif, E-S. M., (2012). *Electrochemical and Gravimetric Study on the Corrosion and Corrosion Inhibition of Pure Copper in Sodium Chloride Solutions by Two Azole Derivatives*, Int. J. Electrochem. Sci., **7**(3), pp. 2374-2388.

11.Cui, Z.-G., Wang, L., Ni, H.-T., Hao, W.-K., Man, Ch., Chen, Sh.-Sh., Wang, X., Liu, Zh.-Y., Li, X.-G., (2017). *Influence of temperature on the electrochemical and passivation behavior of 2507 super duplex stainless steel in simulated desulfurized flue gas condensates*, Corr. Sci., **118**, pp. 31-48, doi: 10.1016/j.corsci.2017.01.016

12.*The Avesta Welding Manual, Practice and products for stainless steel welding*. Available from: http://www.eng.lbl.gov/~shuman/NEXT/MATERIALS&COMPONENTS/Pressure_vessels/ss_weld_manual_avesta.pdf. Accessed: 11/04/2019.

13.Xia, J. Jin, H., (2018). *Numerical analysis for controlling residual stresses in welding design of dissimilar materials girth joints*, H. Int. J. Precis. Eng. Manuf. 2018, **19**(1), pp. 57-66, doi: 10.1007/s12541-018-0007-1

14.Giętka, T., Ciechacki, K., Kik, T., (2016). *Numerical Simulation of Duplex Steel Multipass Welding*, Arch. Metall. Mater., **61**(4), pp. 1975–1984.

15.Wen, P., Song, Y., (2018). *Numerical simulation and process optimization of laser surface treatment on duplex stainless steel*, J. Las. App., **30**(3), pp. 1-7, doi: 10.2351/1.5040646

16. Jyoti V. Menghani, Akshay Govande, Satish R. More, (2017). *Investigation on erosion wear behaviour of Cr_2O_3 plasma thermal spray coating and Ni based hardfacing by welding with Taguchi approach*, International journal of modern manufacturing technologies, **IX**(2), 45-50.

17. Topolska, S., Gwiazda A., (2019). *Properties Analysis of Homogeneous Welding Joints of the Duplex – Austenitic Steel Type Welded with Austenitic Wire*, International Journal of Modern Manufacturing Technologies, **XI**(1), pp. 122-127

Received: April 15, 2019 / Accepted: June 15, 2020 / Paper available online: June 20, 2020